JOURNAL OF GUIDANCE, CONTROL, AND DYNAMICS
Vol. 18, No. 4, July–August 1995

Aircraft Terrain Following Based on a Nonlinear Continuous Predictive Control Approach

Ping Lu* and Bion L. Pierson†
Iowa State University, Ames, Iowa 50011-3231

This paper discusses aircraft terrain-following flight control law development based on a new nonlinear optimal predictive control method. The control law minimizes the predicted difference between the actual trajectory and a smooth open-loop reference trajectory that satisfies the aircraft dynamic model. A fixed-point algorithm is used to compute sequentially the tracking control commands from the implicit control law. Globally asymptotically stable tracking of the reference trajectory is proved in the absence of control saturation, and the influences of the controller parameters on the tracking dynamics are identified. Numerical simulations are presented for a supersonic fighter aircraft model over a standard test terrain. These simulations include the effects of initial condition errors, aerodynamic modeling inaccuracies, and vertical wind disturbances.

Nomenclature

C_L, C_D	= lift and drag coefficients
D	= aerodynamic drag
g	= gravitational acceleration
L	= aerodynamic lift
M	= Mach number
m	= constant mass
Q_1, Q_2	= positive semidefinite weighting matrices
S	= reference area of aircraft
s_1, s_2	= saturation functions
T	= thrust
$T_{\max}$	= maximum thrust
t	= time
$u(t)$	= control vector
x	= state vector
x, y	= dimensional position coordinates
v	= velocity
v_s	= speed of sound at sea level
y	= altitude
α	= angle of attack
γ	= flight-path angle
η	= throttle setting
$\bar{\rho}$	= atmospheric density
ϕ	= specified weighting parameter

I. Introduction

TWO of the major tasks involved in an aircraft terrain-following (TF) problem are trajectory planning and trajectory tracking. In trajectory planning, a reference trajectory is generated offline that follows a given terrain closely and satisfies all of the mission requirements and the aircraft performance constraints.[1] It is then the task of the flight control system to ensure that the aircraft tracks the reference trajectory, even in the presence of off-nominal perturbations and external disturbances. In Refs. 2–4, predictive control techniques are used for this purpose where the aircraft is represented by a linear, discrete-time model. A linear robust control approach called U-parameter design is employed in Ref. 5 where again a linearized, time-invariant model of the aircraft is required. When the flight conditions during terrain following vary significantly, the time-invariance assumption is no longer valid and some type of gain scheduling is necessary.

Alternatively, nonlinear control approaches have also been proposed for the TF problem. Lee et al.[6] apply a nonlinear control technique called optimal decision strategy[7] to the TF control problem. A quadratic programming problem needs to be solved at each instant when the control commands are calculated. This can present a problem for onboard real-time implementation. Rehbock et al.[8] take the same approach but discretize the problem into a sequence of linear programming problems. The control commands are obtained as a sequence of data points indexed by time; thus, the controls are open loop in nature. Barnard[9] points out some disadvantages of the latter two schemes and proposes an approach based on an optimal aim strategy concept. However, all three of these methods require the controls to appear linearly in the (nonlinear) system equations. Since the point-mass model of an aircraft does not naturally meet this requirement, a transformation must be applied to redefine the controls to fit the required form.[6] This causes some unintended degradation of control effectiveness by these schemes when the controls saturate. This aspect will be discussed further at the end of Sec. III.

This paper constitutes the second part of our work on the aircraft terrain-following problem. The first part of the work on optimal trajectory analysis and generation is reported in Ref. 1. This paper addresses the issue of tracking control law development for the aircraft to follow a predesigned TF trajectory. It is assumed that mission requirements demand very accurate tracking of the reference TF trajectory. Continued improvements in terrain modeling and precision navigation are expected to lead to significant reduction in terrain clearance altitude of the reference trajectory.[10] In such a case, the tracking accuracy of the flight control system will be the limiting factor in performance. It is this anticipated stringent performance requirement that justifies the study presented here.

We first introduce a general continuous nonlinear predictive control method in Sec. II. A feedback control law is obtained as a result of a pointwise minimization of the difference between the predicted system response and the desired response. The approach is then applied to the TF control problem in Sec. III. Globally asymptotic tracking of the reference trajectory under the predictive controller is analytically studied to validate the use of the technique. An efficient fixed-point algorithm is utilized for onboard computation of the control commands. The effectiveness and robustness of the controller are tested in simulations under a variety of trajectory dispersions and disturbances for a supersonic fighter aircraft model in Sec. IV. Finally, the main conclusions are summarized in Sec. V.

II. Nonlinear Continuous Predictive Control Laws

Consider a nonlinear dynamic system of the general form

$$\dot{x}_1 = f_1(x) \tag{1}$$

Received Aug. 4, 1994; revision received Nov. 5, 1994; accepted for publication Nov. 5, 1994; presented as Paper 95-3342 at the AIAA Guidance, Navigation, and Control Conference, Baltimore, MD, Aug. 7–9, 1995.

*Associate Professor, Department of Aerospace Engineering and Engineering Mechanics. Senior Member AIAA.

†Professor, Department of Aerospace Engineering and Engineering Mechanics. Associate Fellow AIAA.

$$\dot{x}_2 = f_2(x) + g_2(x, u) \tag{2}$$

where the state vector is $x = (x_1^T x_2^T)^T \in R^n$ with $x_1 \in R^{n_1}, x_2 \in R^{n_2}$, and $n_1 + n_2 = n$. The control vector is $u(t) \in U = \{u(t) \in R^m | L_i \le u_i(t) \le U_i\}$ with the bounds L_i and U_i specified. The functions f_1: $R^n \to R^{n_1}$, f_2: $R^n \to R^{n_2}$ and g_2: $R^n \times R^m \to R^{n_2}$ are continuously differentiable nonlinear functions. Suppose that the desired response of the system is described by a reference history $x^*(t)$ of the state $x(t)$. More specifically, we assume the following.

Assumption: A desired trajectory $x^*(t) \in R^n$, $t \in [0, t_f]$, and the corresponding control $r^*(t) \in U$ are known, and $x^*(t)$ and $r^*(t)$ satisfy the system Eqs. (1) and (2).

This assumption assures that the desired response is within the performance capabilities of the system, which is certainly the case for terrain-following control problems when the reference trajectory is generated based on the dynamic model of the aircraft. To design a feedback control law for $u(t)$ so that the system response $x(t)$ tracks $x^*(t)$ for some arbitrary initial conditions, a continuous predictive control concept is developed in Refs. 11–13. For completeness, a brief outline of the approach is given here. Suppose that at an arbitrary $t \in [0, t_f]$, $\ddot{x}_1(t)$ and $\dot{x}_2(t)$ depend on the control $u(t)$ explicitly. More general situations can be treated similarly,[11] but this suffices for the TF problem. Then, the choice of $u(t)$ will influence the response of the system at the next instant. In particular, for a small time increment $\delta > 0$, by expanding $x_1(t + \delta)$ in a second-order Taylor series expansion and $x_2(t + \delta)$ in a first-order expansion

$$x_1(t + \delta) \approx x_1(t) + \delta f_1[x(t)] + (\delta^2/2)\{F_{11}[x(t)]f_1[x(t)] + F_{12}[x(t)]f_2[x(t)] + F_{12}[x(t)]g_2[x(t), u(t)]\} \tag{3}$$

$$x_2(t + \delta) \approx x_2(t) + \delta\{f_2[x(t)] + g_2[x(t), u(t)]\} \tag{4}$$

we can see the effect of $u(t)$ on $x_1(t + \delta)$ and $x_2(t + \delta)$ more clearly. In Eq. (3), $F_{11}(x) = \partial f_1[x(t)]/\partial x_1$ and $F_{12}(x) = \partial f_1[x(t)]/\partial x_2$ where the derivative of each component of f_1 with respect to x is defined as a row vector. Also, partition $x^*(t)$ accordingly into $[x_1^{*T}(t) x_2^{*T}(t)]^T$ and similarly expand $x_1^*(t + \delta)$ and $x_2^*(t + \delta)$ to obtain

$$x_1^*(t + \delta) \approx x_1^*(t) + \delta\dot{x}_1^*(t) + (\delta^2/2)\ddot{x}_1^* \tag{5}$$

$$x_2^*(t + \delta) \approx x_2^*(t) + \delta\dot{x}_2^* \tag{6}$$

The tracking error at $t + \delta$ can then be approximated by

$$e_1(t + \delta) = x_1(t + \delta) - x_1^*(t + \delta) \approx e_1(t) + \delta\dot{e}_1(t) + 0.5\delta^2 \times [F_{11}(x)f_1(x) + F_{12}(x)f_2(x) + F_{12}(x)g_2(x, u) - \ddot{x}_1^*] \tag{7}$$

$$e_2(t + \delta) = x_2(t + \delta) - x_2^*(t + \delta) \approx e_2(t) + \delta(f_2(x) + g_2(x, u) - \dot{x}_2^*) \tag{8}$$

where the dependence of $x(t)$, $x^*(t)$, and $u(t)$ on t has been suppressed for simplicity. Assume that $x(t)$ is known. The control $u(t)$ is chosen to minimize the performance index

$$\min_{u \in U} J = \min_{u \in U} \tfrac{1}{2}e_1^T(t + \delta)Q_1e_1(t + \delta) + \tfrac{1}{2}e_2^T(t + \delta)Q_2e_2(t + \delta) + \tfrac{1}{2}[u(t) - r^*(t)]^T R[u(t) - r^*(t)] \tag{9}$$

where Q_1 and Q_2 are positive semidefinite matrices with appropriate dimensions. $R \in R^{m \times m}$ is positive definite when $g_2(x, u)$ is nonlinear in u and can be set to zero when $g_2(x, u)$ is linear in u, namely, when Eq. (2) is

$$\dot{x}_2 = f_2(x) + B_2(x)u \tag{10}$$

In this case, a closed-form solution for the control $u(t)$ can be obtained by setting $\partial J/\partial u(t) = 0$ in the absence of control saturations[11,12]:

$$u(t) = -P^{-1}\{(1/2\delta^2)(F_{12}B_2)^T Q_1[e_1 + \delta\dot{e}_1 + (\delta^2/2)(F_{11}f_1 + F_{12}f_2 - \ddot{x}_1^*)] + (1/\delta^2)B_2^T Q_2[e_2 + \delta(f_2 - \dot{x}_2^*)]\} \tag{11}$$

where

$$P = [0.25(F_{12}B_2)^T Q_1 F_{12}B_2 + (1/\delta^2)B_2^T Q_2 B_2] \tag{12}$$

and where all the quantities are evaluated at time t.

When the system is nonlinear in u, setting $\partial J/\partial u(t) = 0$ with a positive definite R yields

$$u(t) = r^*(t) - hR^{-1}\left\{0.5h\left(F_{12}(x)\frac{\partial g_2(x, u)}{\partial u}\right)^T \times Q_1[e_1 + h\dot{e}_1 + 0.5h^2(F_{11}(x)f_1(x) + F_{12}(x)f_2(x) + F_{12}(x)g_2(x, u) - \ddot{x}_1^*)] + \left(\frac{\partial g_2(x, u)}{\partial u}\right)^T \times Q_2[e_2(t) + h(f_2(x) + g_2(x, u) - \dot{x}_2^*)]\right\} \triangleq \rho(u) \tag{13}$$

where $\rho(\cdot)$ is used to represent the nonlinear mapping on u defined by the right-hand side of Eq. (13). A continuous implicit feedback control law is defined by Eq. (13). To account for the possible control saturations, we define the vector saturation function $s(y) = [s_1(y) \cdots s_m(y)]^T$ for any $y \in R^m$ as

$$s_i(y) = \begin{cases} U_i, & y_i \ge U_i \\ y_i, & L_i < y_i < U_i \\ L_i, & y_i \le L_i \end{cases} \tag{14}$$

for $1 \le i \le m$. Then apply this saturation function to the right-hand side of Eq. (13) to ensure $u \in U$

$$u = s[\rho(u)] \tag{15}$$

In this case no closed-form solutions for $u(t)$ from Eq. (15) exist in general. Nonetheless, the following result is obtained in Ref. 13 regarding the existence and uniqueness of the solution of Eq. (15) and how to find it.

Theorem 1: At any $t \in [0, t_f]$, for any given bounded values of $x(t), x^*(t), r^*(t)$, $Q_1 \ge 0$, $Q_2 \ge 0$, and $R > 0$, there always exists a sufficiently small $\delta_0 > 0$ such that for all $0 < \delta \le \delta_0$ the following holds true.

1) The implicit equation (15) has a unique solution $u^* \in U$. When u^* is in the interior of U, it is the unique optimal solution of the problem (9).

2) Furthermore, define a ball $B_\epsilon = \{u \in R^m | \|u - r^*\| \le \varepsilon\}$ for some $\varepsilon > 0$. Then, the fixed-point iteration sequence $\{u^k\}$ generated by

$$u^k = s[\rho(u^{k-1})], \qquad k = 1, 2, \ldots, \qquad \forall u^0 \in B_\epsilon \tag{16}$$

converges to u^*.

The fixed-point iteration algorithm (16) is the key that makes the control law (15) potentially useful for online applications because fixed-point iteration is particularly well suited for digital computers and the iteration (16) converges usually in just a few cycles. Discussion on general properties of the control laws (11) and (15) can be found in Refs. 11–13. For the application in this paper, we only state two such properties here. First, it can be shown that if at any $t_0 \in [0, t_f]$ the tracking error $e(t_0) = x(t_0) - x^*(t_0) = 0$, then $e(t) \equiv 0$ for all $t \in [t_0, t_f]$ under control law (11) or (15). In other words, perfect tracking will be maintained once achieved, provided there are no further perturbations and disturbances. Second, the parameter δ should not be regarded as the integration step size. In fact, it can be tuned independently as a controller parameter for better performance. It has been found that a good value of δ in control law (15) should be typically an order of magnitude greater than the integration step size used in the simulation, as long as it is still sufficiently small for the fixed-point iteration (16) to converge.

III. Aircraft Terrain-Following Flight Control

Equations of Motion and Reference Trajectory

In a TF problem, it is natural to use the down range distance as the independent variable. Following the formulation in Ref. 1, we have the aircraft point-mass equations of motion in a vertical plane over a flat Earth

$$\frac{dh}{dX} = \tan\gamma \tag{17}$$

$$\frac{dV}{dX} = (A_T\cos\alpha - A_D - \sin\gamma)\frac{1}{V\cos\gamma} \tag{18}$$

$$\frac{d\gamma}{dX} = (A_T\sin\alpha + A_L - \cos\gamma)\frac{1}{V^2\cos\gamma} \tag{19}$$

where all of the variables are dimensionless and defined by

$$h = gy/v_s^2, \qquad X = gx/v_s^2, \qquad V = v/v_s \tag{20}$$

$$A_T = T/mg, \qquad A_D = D/mg, \qquad A_L = L/mg \tag{21}$$

The thrust T is modeled by

$$T = T_{\max}(M, y)\eta \tag{22}$$

In general, the maximum thrust $T_{\max}$ is a function of Mach number M and altitude y. L and D are the aerodynamic lift and drag, respectively,

$$L = qSC_L, \qquad D = qSC_D \tag{23}$$

and $q = \bar{\rho}v^2/2$ is the dynamic pressure with atmospheric density $\bar{\rho}$ which is assumed to be an exponential function of the altitude y with the scale height equal to 23,800 ft. The lift and drag coefficients, C_L and C_D, are functions of the angle of attack α and Mach number M. The throttle setting η and angle of attack α are taken as the controls.

Suppose that the terrain elevation plus a set clearance at the distance X is given by a smooth function $F(X)$. The initial conditions and terminal constraints on the aircraft trajectory are specified as

$$h(0) = h_0, \qquad V(0) = V_0, \qquad \gamma(0) = \gamma_0 \tag{24}$$

$$\Psi[h(X_f), V(X_f), \gamma(X_f)] = \mathbf{0} \tag{25}$$

Equations (25) represent a system of $r \leq 3$ algebraic equations that specify the terminal state constraints. The constraints on the controls are

$$0 \leq \eta_{\min} \leq \eta \leq \eta_{\max} \leq 1.0 \qquad \text{and} \qquad \alpha_{\min} \leq \alpha \leq \alpha_{\max} \tag{26}$$

The reference terrain-following trajectory is obtained as a solution of the optimal control problem in which the performance index

$$J = \int_0^{X_f}\left\{\phi\left(\frac{1}{V\cos\gamma}\right) + (1-\phi)[h - F(X)]^2\right\}dX \tag{27}$$

$$0 < \phi < 1.0$$

is minimized, where the integral of the first term in Eq. (27) is the time of flight. Therefore, along the optimal trajectory, the aircraft will follow the terrain closely and fly fast.[1] In Ref. 1, it has been shown that for a rather general class of aircraft models the optimal solution always calls for bang-bang throttle control, and by using an inverse dynamics approach we can obtain the optimal solution very reliably and efficiently.

Validation of Flight Control Approach

The nonlinear continuous predictive control approach introduced in Sec. II will now be used for terrain-following flight control. To validate the approach, we shall show that the minimization of the local predicted tracking errors [Eq. (9)] will indeed lead to globally asymptotic tracking of the reference TF trajectory. For the purpose of proof of the concept, we find it more convenient to use control law (11). In this regard, we redefine the controls as

$$u_1 = A_T\cos\alpha - A_D \tag{28}$$

$$u_2 = A_T\sin\alpha + A_L \tag{29}$$

The effectiveness of the proposed control approach is summarized in the following Theorem.

Theorem 2: Let an arbitrary reference TF trajectory be denoted by $[h^*(X)\ V^*(X)\ \gamma^*(X)]$ which satisfies the Assumption in Sec. II. Let $Q_1 = Q_h$, $Q_2 = \text{diag}\{Q_V, Q_\gamma\}$ and $\boldsymbol{R} = 0$ in the performance index J defined in Eq. (9). Then, for any $\delta > 0$, $Q_h > 0$, $Q_V > 0$, and $Q_\gamma > 0$, the controls u_1 and u_2 obtained by minimizing J guarantee globally asymptotically stable tracking of the reference trajectory in the absence of control saturations.

Proof: To conform to the notation in Sec. II, we denote $x_1 = h$ and $x_2 = (V\tan\gamma)^T$, where we use $\tan\gamma$ instead of γ itself because this simplifies the proof significantly. (Since $|\gamma| < 90$ deg, proving $\tan\gamma \to \tan\gamma^*$ is equivalent to showing $\gamma \to \gamma^*$.) With u_1 and u_2 defined in Eqs. (28) and (29), the state equations (17–19) become

$$\frac{dh}{dX} = \tan\gamma \tag{30}$$

$$\frac{dV}{dX} = -\frac{\tan\gamma}{V} + \left[\frac{1}{V}\sqrt{1+\tan^2\gamma}\right]u_1 \tag{31}$$

$$\frac{d(\tan\gamma)}{dX} = -\frac{1}{V^2}(1+\tan^2\gamma) + \left[\frac{1}{V^2}\sqrt{(1+\tan^2\gamma)^3}\right]u_2 \tag{32}$$

In the absence of control saturations, minimization of J in Eq. (9) with respect to u_1 and u_2 leads to the control law (11). Applying Eq. (11) to system (30–32) gives

$$u_1 = V\cos\gamma\left(\frac{1}{V}\tan\gamma + \dot{V}^* - \frac{1}{\delta}\Delta V\right) \tag{33}$$

$$u_2 = -\frac{\delta V^2\cos^3\gamma}{0.25Q_h\delta^2 + Q_\gamma}\left\{\frac{Q_h}{2\delta}(\Delta h + \delta\Delta\dot{h}) - 0.25Q_h\delta\left(\frac{1+\tan^2\gamma}{V^2} + \ddot{h}^*\right) + \frac{Q_\gamma}{\delta^2}\left[\Delta\tan\gamma - \delta\left(\frac{1+\tan^2\gamma}{V^2} + \frac{\dot{\gamma}^*}{\cos^2\gamma^*}\right)\right]\right\} \tag{34}$$

where the dot indicates differentiation with respect to X, and Δ in front of a quantity means the difference between the actual and reference values of that quantity. Substituting (33) and (34) back into Eqs. (31) and (32), respectively, we have the error equations

$$\Delta\dot{V} = -(1/\delta)\Delta V \tag{35}$$

$$\frac{d(\Delta\tan\gamma)}{dX} = -\frac{\delta}{0.25Q_h\delta^2 + Q_\gamma} \times\left\{\frac{Q_h}{2\delta}(\Delta h + \delta\Delta\dot{h}) + \frac{Q_\gamma}{\delta^2}\Delta\tan\gamma\right\} \tag{36}$$

where in arriving at Eq. (36), the relationship $\ddot{h}^* = d(\tan\gamma^*)/dX$ has been used since the reference h^* and γ^* satisfy the state equation (30) by the Assumption. It is clear now from Eq. (35) that the velocity error $\Delta V \to 0$ for any $\delta > 0$. Since $\Delta\tan\gamma = \Delta\dot{h}$ and $d(\Delta\tan\gamma)/dX = \Delta\ddot{h}$, Eq. (36) is the same as

$$(0.25\delta^2Q_h + Q_\gamma)\Delta\ddot{h} + [0.5\delta Q_h + (Q_\gamma/\delta)]\Delta\dot{h} + 0.5Q_h\Delta h = 0 \tag{37}$$

Obviously, for any $Q_h > 0$, $Q_\gamma > 0$, and $\delta > 0$, the preceding second-order system is stable; therefore, $\Delta h \to 0$, and thus $\Delta\tan\gamma \to 0$ for any initial conditions. Hence, globally asymptotically stable tracking of the reference trajectory is achieved. As for the corresponding physical controls η and α, they can always be

solved numerically from Eqs. (28) and (29) for u_1 and u_2 given in Eqs. (33) and (34) since by assumption no saturation occurs.

The proof also offers some interesting interpretations of the roles of the controller parameters δ, Q_h, and Q_γ. From Eq. (35), δ turns out to be simply the time constant of the closed-loop velocity dynamics. The choice of $Q_V > 0$ is immaterial because it does not appear in the control law. For given δ, values Q_h and Q_γ determine the damping and natural frequency of the altitude dynamics. For instance, in the terrain-following problem, overshoots in Δh (i.e., $\Delta h < 0$) should be avoided whenever possible because the terrain is rather unforgiving. Thus, the damping ratio of the altitude dynamics is best set at unity (critical damping) to eliminate overshoot and still provide fast response. By Eq. (37), this requires

$$\frac{Q_h}{Q_\gamma} = \frac{2(\sqrt{2}-1)}{\delta^2} \tag{38}$$

This relationship will later serve as a guide for choosing the values of Q_h and Q_γ.

Although control law (11) is used successfully to demonstrate the validity of the control approach, it is inconvenient to apply to the aircraft TF control problem for two reasons: 1) Once the fictitious controls u_1 and u_2 are computed from Eqs. (33) and (34), the physical controls α and η still need to be solved for iteratively from Eqs. (28) and (29) because A_L and A_D depend on α. 2) The control constraints on α and η are not easy to enforce in terms of simple constraints on u_1 and u_2. Therefore in the actual implementation, the implicit control laws (15) for α and η, which handle control constraints effortlessly and are suited for the fixed-point iteration algorithm (16), appear to be a better alternative and are, thus, used in the next section.

It should be pointed out that in Ref. 6 the aircraft thrust is assumed to be aligned with the velocity vector, and a similar transformation is applied so that the system equations are linear in the two controls, C_L and τ^*, where τ^* is a combination of thrust and drag forces. This results in the bounds of τ^* depending on the first control C_L. On the basis of this formulation, Refs. 6 and 9 solve a quadratic programming problem with respect to the controls at each instant, and Ref. 8 solves a linear programming problem. When τ^* saturates, however, the problem formulations are neither linear nor quadratic programming problems,[14] because of the dependence of the bounds of one control on the other control. This complication appears to be unavoidable when transforming a constrained physical system that is nonlinear in the controls into one which is linear in the controls.

IV. Numerical Simulations

A supersonic fighter aircraft model given in Ref. 15 (airplane 2) is used for the numerical experiments. The lift and drag coefficients of the aircraft have the functional forms

$$C_L = C_{L\alpha}\alpha \tag{39}$$

$$C_D = C_{D0} + C_{L\alpha}\alpha^2 \tag{40}$$

where $C_{L\alpha}$ and C_{D0} are originally given in tabulated data as functions of Mach number M and are fitted by least-square polynomials for $0 \le M \le 2.4$ in this study:

$$C_{L\alpha} = 2.2371 + 0.34008M - 0.2615M^2 + 0.01085M^3 \tag{41}$$

$$C_{D0} = 0.0065 - 0.0022187M - 0.01649M^2 + 0.043848M^3 - 0.028402M^4 + 0.005493M^5 \tag{42}$$

The bounds on the two controls α, in degrees, and η are set at

$$\alpha_{\max} = 20, \qquad \alpha_{\min} = -10 \tag{43}$$

$$\eta_{\max} = 1.0, \qquad \eta_{\min} = 0.0 \tag{44}$$

The maximum thrust $T_{\max}$ of the aircraft is given in tabular form as a function of altitude and Mach number.[15] Linear interpolations are used here for table look-up evaluations of $T_{\max}$. The weight of the aircraft is set at 34,000 lb and is considered constant. A reference TF trajectory is taken to be an optimal trajectory obtained by using the inverse dynamics approach in Ref. 1. The boundary conditions of the reference trajectory in terms of the dimensional variables are

$$y(0) = 200, \quad \gamma(0) = 0, \quad v(0) = 557.5\,(M = 0.5) \tag{45}$$

$$y(x_f) = 640, \quad \gamma(x_f) = 0, \quad v(x_f) = 1114.9\,(M = 1.0) \tag{46}$$

where y is given in feet, γ in degrees, and v in feet per second and $x_f = 65{,}000$ ft. The terrain function $F(X)$ is the same one used in Ref. 1. The performance index for the reference trajectory is given in Eq. (27) with $\phi = 0.5$. In generating the reference trajectory, we limit the throttle setting by $0.3 \le \eta \le 0.7$. This is done because the optimal throttle setting is of bang-bang type,[1] and such limits prevent the aircraft from always operating at full throttle or idling the engine along the nominal TF trajectory. Also it gives the trajectory tracking some leeway in control authority when needed. The optimal trajectory takes 70.7 s of flight for the preceding boundary conditions, and the terrain is followed perfectly.

Let $Q_1 = Q_h$, $\boldsymbol{Q}_2 = \mathrm{diag}\{Q_V, Q_\gamma\}$, $\boldsymbol{R} = \mathrm{diag}\{R_1, R_2\}$. The tracking control laws for η and α by following Eqs. (13) and (15) are

$$\eta = s_1\Bigg(\eta^* - \frac{\delta}{R_1}\Bigg\{PA_{T_{\max}}\sin\alpha + G_{11}Q_V\Bigg[\Delta V + \eta\Bigg(\frac{A_T\cos\alpha - A_D}{V\cos\alpha} - \frac{\tan\gamma}{V} - \dot{V}^*\Bigg)\Bigg] + G_{21}Q_\gamma\Bigg[\Delta\gamma + \delta\Bigg(\frac{A_T\sin\alpha + A_L}{V^2\cos\gamma} - \frac{1}{V^2} - \dot{\gamma}^*\Bigg)\Bigg]\Bigg\}\Bigg) \tag{47}$$

$$\alpha = s_2\Bigg(\alpha^* - \frac{\delta}{R_2}\Bigg\{P\big(A_T\cos\alpha + qSC_{L_\alpha}\big) + G_{12}Q_V\Bigg[\Delta V + \delta\Bigg(\frac{A_T\cos\alpha - A_D}{V\cos\alpha} - \frac{\tan\gamma}{V} - \dot{V}^*\Bigg)\Bigg] + G_{22}Q_\gamma\Bigg[\Delta\gamma + \delta\Bigg(\frac{A_T\sin\alpha + A_L}{V^2\cos\gamma} - \frac{1}{V^2} - \dot{\gamma}^*\Bigg)\Bigg]\Bigg\}\Bigg) \tag{48}$$

where s_1 and s_2 are the saturation functions defined in Eq. (14) and

$$P = \frac{0.5\delta Q_h}{V^2\cos^3\gamma}\Bigg[\Delta h + \delta\Delta\dot{h} + 0.5\delta^2\Bigg(-\frac{1}{V^2\cos^2\gamma} + \frac{A_T\sin\alpha + A_L}{V^2\cos^3\gamma} - \ddot{h}^*\Bigg)\Bigg] \tag{49}$$

$$G_{11} = \frac{A_{T_{\max}}\cos\alpha}{V\cos\gamma}, \qquad G_{12} = -\frac{1}{V\cos\gamma}\big(A_T\sin\alpha + 2qSC_{L_\alpha}\alpha\big) \tag{50}$$

$$G_{21} = \frac{A_{T_{\max}}\sin\alpha}{V^2\cos\gamma}, \qquad G_{22} = \frac{1}{V^2\cos\gamma}\big(A_T\cos\alpha + qSC_{L_\alpha}\big) \tag{51}$$

The values of the controller parameters are chosen to be

$$\delta = 0.005, \qquad Q_V = Q_\gamma = 1.0, \qquad Q_h = 30000$$
$$R_1 = 0.001, \qquad R_2 = 0.2 \tag{52}$$

where the value of δ corresponds to about 193 ft in dimensional distance. For $Q_\gamma = 1$ and $\delta = 0.005$, Eq. (38) gives $Q_h = 33137$, which indicates the order of magnitude that Q_h should have. Some minor adjustments may need to be made through simulations because the control laws (47) and (48) are not exactly the same as Eqs. (33) and (34). In particular, $\boldsymbol{R} = 0$ in Eqs. (33) and (34) whereas $\boldsymbol{R} > 0$ is required in Eqs. (47) and (48). The guidelines are that a larger Q_h gives a tighter altitude control but may cause overshoot, and a larger Q_γ increases the damping of the altitude dynamics. The path-tracking performance of the controller is not influenced

to any significant extent by the choice of Q_V (recall the discussion after Theorem 2 in Sec. III). The value of $Q_h = 33137$ is found to produce a slight overshoot in Δh. The simulation is performed with a standard fourth-order Runge–Kutta routine with an integration step size of 0.0001 (dimensionless). The controls η and α are solved from Eqs. (47) and (48) by fixed-point iterations every time when the right-hand sides of the equations of motion are evaluated in the simulation.

The first test is on the performance of the control approach in the presence of initial trajectory dispersions. Note that the reference trajectory will be tracked perfectly if there are no trajectory dispersions and disturbances under the current control laws. Two sets of off-nominal initial conditions are created with y in feet, v in feet per second, and γ in degrees.

Case 1:

$$\Delta y(0) = 600, \qquad \Delta v(0) = 557.5, \qquad \Delta\gamma(0) = 10 \tag{53}$$

Case 2:

$$\Delta y(0) = 1400, \qquad \Delta v(0) = 0, \qquad \Delta\gamma(0) = 0 \tag{54}$$

Figure 1 shows the altitude histories. It is seen that in spite of the large initial dispersions, the trajectories quickly converge onto the reference path gracefully. The tracking errors at $x_f = 65{,}000$ ft are, for case 1 and case 2 (retaining the preceding units), respectively,

$$\Delta y_f = 0.07, \qquad \Delta v_f = 4.8, \qquad \Delta\gamma_f = 0.0003$$

$$\Delta y_f = 0.03, \qquad \Delta v_f = 4.2, \qquad \Delta\gamma_f = -0.0002$$

Figures 2 and 3 give the corresponding control histories of α and η. Note that both controls are saturated at the beginning where the initial errors are large. If the saturations are not desired, increasing the values of R_1 and R_2 in the control laws (47) and (48) can reduce or eliminate them effectively. The consequence, of course, is that the convergence to the reference trajectory will be slower. The number of fixed-point iterations at each step is mostly one for an accuracy of 10^{-4} for both controls, except for a few initial points where the number of iterations ranges from 3 to 4.

It should be pointed out that although the control laws (47) and (48) are derived based on a point-mass model of the aircraft, the methodology is equally applicable when rotational dynamics and engine dynamics are included. Although the computation requirements appear to be relatively minor as already indicated, since this first effort is aimed at using a continuous predictive control method for TF control law development, we have not addressed the important issues of flight control system implementation. Specifically, the integration of stability augmentation and command-tracking systems and the requirements on sensor and state estimation systems remain to be investigated.

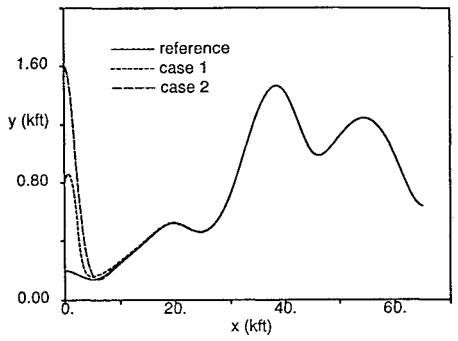

Fig. 1 Altitude tracking histories.

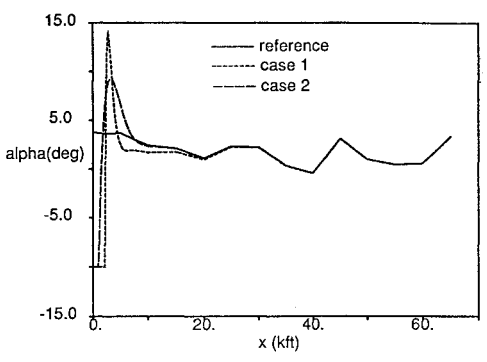

Fig. 2 Angle-of-attack histories.

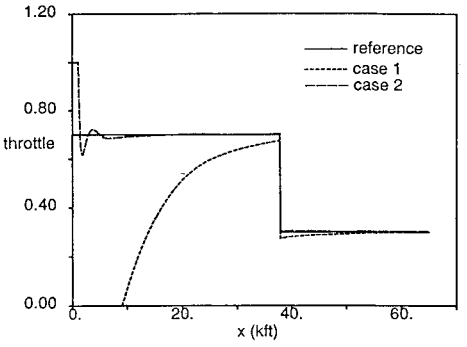

Fig. 3 Throttle setting histories.

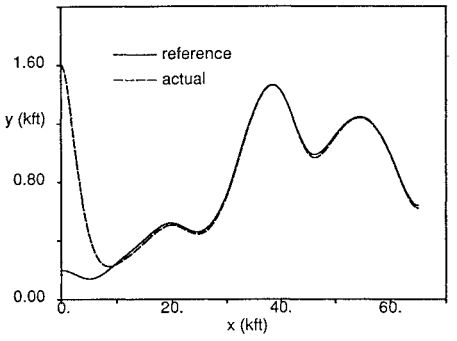

Fig. 4 Altitude tracking history in the presence of aerodynamic modeling inaccuracies.

Since the controls are obtained by continuously minimizing the predicted tracking errors, the controller is expected to have reasonable robustness, provided accurate state feedback is available. To test the robustness of the controller, we consider aerodynamic modeling inaccuracies and external disturbances. For instance, we set the aerodynamic coefficients in the simulation of the aircraft motion to be

$$C_{L_\alpha} = 0.7C^*_{L_\alpha}, \qquad C_{D0} = 2C^*_{D0} \tag{55}$$

where the values with asterisk are the nominal ones given by Eqs. (41) and (42). In the computation of η and α, only the nominal values of C_{L_α} and C_{D0} are assumed, but accurate current values of h, V, and γ are used. To compensate the reduction in C_L which affects the flight path the most at low speeds, the value of Q_γ is increased to 2.0 so that no significant overshoot in Δy will occur. The altitude history for the initial conditions (54) is plotted in Fig. 4. If Q_γ is still set at unity, most of the trajectory is about the same, except that the peak overshoot in Δy is larger (not shown in the figure). When the aircraft flies at high speeds [for example, taking initial conditions (53)], then the trajectory is almost indiscernible from the one without aerodynamic modeling inaccuracies. The reaction of the controller to the inaccuracies can be clearly seen in Figs. 5 and 6 in which higher angle of attack and throttle setting are recorded to account for lower C_L and higher C_D. Also plotted in Fig. 5 is the variation of the pitch angle of the aircraft, $\theta = \alpha + \gamma$, which first shows a quick dive to catch the terrain from the initial altitude and then adjusts to track the terrain.

One possible external disturbance is wind. The presence of a wind alters the equations of motion of the aircraft. Let us consider a vertical wind the (dimensionless) speed of which at the

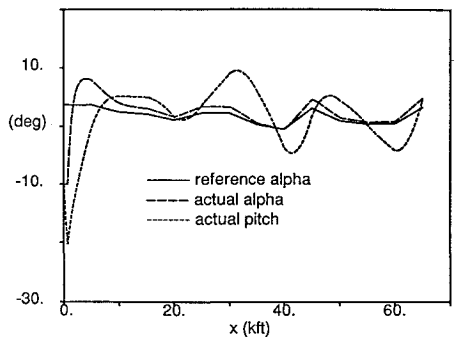

Fig. 5 Angle-of-attack and pitch angle histories in the presence of aerodynamic modeling inaccuracies.

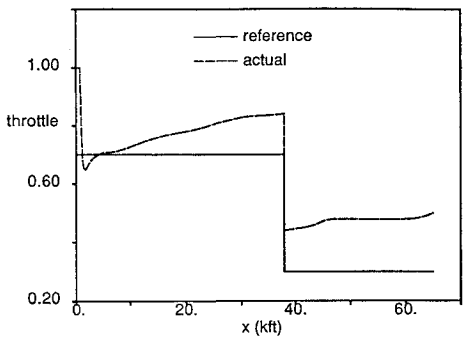

Fig. 6 Throttle setting history in the presence of aerodynamic modeling inaccuracies.

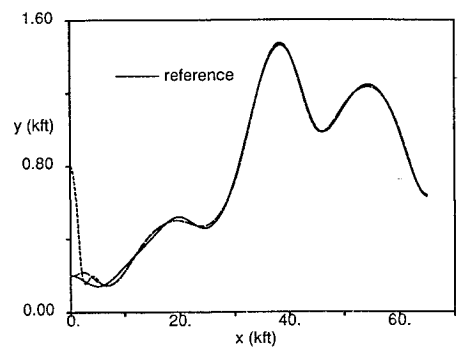

Fig. 7 Altitude tracking histories in the presence of vertical wind.

distance X is represented by $W(X)$. The equations of motion now become[16]

$$\frac{dh}{dX} = \tan\gamma + \frac{W}{V\cos\gamma} \tag{56}$$

$$\frac{dV}{dX} = (A_T\cos\alpha - A_D - \sin\gamma)\frac{1}{V\cos\gamma} - W_X\sin\gamma \tag{57}$$

$$\frac{d\gamma}{dX} = (A_T\sin\alpha + A_L - \cos\gamma)\frac{1}{V^2\cos\gamma} - \frac{W_X\cos\gamma}{V} \tag{58}$$

where $W_X = \partial W/\partial X$. Instead of relying on knowledge of the wind distribution which is difficult to get, we simply treat the terms dependent on W as uncertainties. As a test, a vertical wind speed profile is specified as

$$W = W_0\sin[(2x/3500)\pi] \tag{59}$$

where $W_0 = 60$ ft/s and x is in feet. The controller is given no information about the wind. For a tighter trajectory control, Q_h is increased to 500,000 and Q_γ is kept at 2.0. The value of δ is set at 0.0025. [In the presence of system uncertainties, Eq. (38) is less accurate a guide for selecting the parameters. But the guidelines mentioned earlier are still applicable.] Figure 7 shows two altitude histories, one with no initial errors and the other with $\Delta y(0) =$

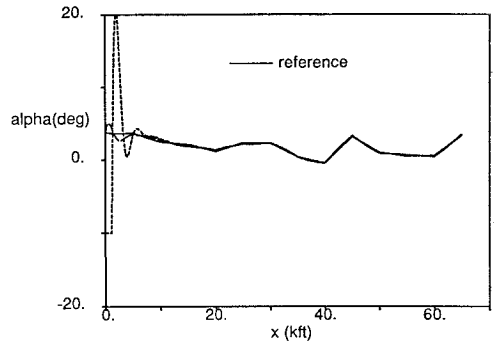

Fig. 8 Angle-of-attack histories in the presence of vertical wind.

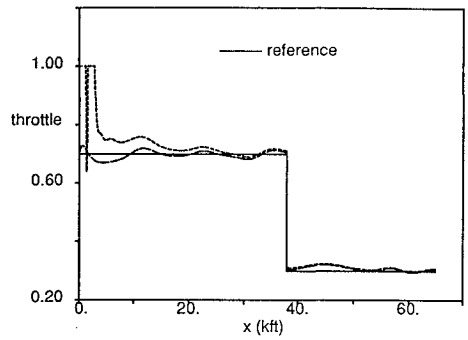

Fig. 9 Throttle setting histories in the presence of vertical wind.

600 ft. In the presence of such a fairly strong wind, the reference TF trajectory is still tracked closely for the most part. The control histories are given in Figs. 8 and 9. The influence of the sinusoidal wind is more profound on the throttle setting. Further adjusting the controller parameters does not seem to improve the performance noticeably. If some information about the wind is available and incorporated into the controller, the overshoot/undershoot phenomenon in the initial portion of the trajectory seen in Fig. 7 can be further reduced.

From the simulations, the controller appears to work remarkably well in the nominal situation. We also wish to point out that because of the very stringent requirement of avoiding a crash with the terrain while trying to follow it closely, the terrain-tracking problem is much more challenging than other trajectory tracking problems in the face of disturbances and uncertainties. In the preceding simulations, if the parameter adjustments are not done, the controller is sufficiently robust so that the trajectory will still eventually follow the reference trajectory very closely. This may be satisfactory for other applications, but not the terrain-following problem, since the transient response has large overshoots in Δy. Although this study shows that appropriate tuning of the controller can produce accurate robust terrain tracking, methods for automated self-tuning of the controller based on available information are still open to future research.

V. Conclusions

This paper considers the flight control law development for an aircraft to track a terrain-following reference trajectory which is designed offline. A nonlinear continuous predictive control approach is introduced for the feedback control law synthesis. This approach handles control constraints conveniently, and the control commands are obtained reliably by a fixed-point iteration algorithm. The amount of computation required is minimal. The validity of this control approach for the terrain-following control problem is established by showing analytically that globally asymptotically stable tracking of a terrain-following reference trajectory can be achieved, provided no control saturations are encountered. Guidelines for tuning the controller parameters to ensure good terrain tracking are obtained. Numerical simulation results show that under a variety of off-nominal perturbations and a strong vertical wind, the proposed controller proves to be quite effective and robust, even in the

presence of control saturation. The issue of integration of this TF tracking controller with stability augmentation system, however, is left for further investigation.

References

[1]Lu, P., and Pierson, B. L., "Optimal Aircraft Terrain-Following Analysis and Trajectory Generation," *Journal of Guidance, Control, and Dynamics*, Vol. 18, No. 3, 1995, pp. 555–560.

[2]Hess, R. A., and Jung, Y. C., "An Application of Generalized Predictive Control to Rotorcraft Terrain-Following Flight," *IEEE Transactions on Systems, Man, and Cybernetics*, Vol. 19, No. 5, 1989, pp. 955–962.

[3]Jung, Y. C., and Hess, R. A., "Precise Flight-Path Control Using a Predictive Algorithm," *Journal of Guidance, Control, and Dynamics*, Vol. 14, No. 5, 1991, pp. 936–942.

[4]Reid, J. G., Chaffin, D. E., and Silverthorn, J. T., "Output Predictive Algorithmic Control: Precision Tracking with Application to Terrain Following," *Journal of Guidance and Control*, Vol. 4, No. 5, 1981, pp. 502–509.

[5]Wei, Y., Shen, C.-L., and Dorato, P., "*U*-Parameter Design for Terrain-Following Flight Control," *Journal of Guidance, Control, and Dynamics*, Vol. 16, No. 2, 1993, pp. 387–389.

[6]Lee, S. M., Bien, Z., and Park, S. O., "On-Line Optimal Terrain-Tracking System," *Optimal Control Applications and Methods*, Vol. 11, No. 4, 1989, pp. 289–306.

[7]Spong, M. W., Thorp, J. S., and Kleinwaks, J. M. M., "The Control of Robot Manipulators with Bounded Input," *IEEE Transactions on Automatic Control*, Vol. AC-31, No. 6, 1986, pp. 483–490.

[8]Rehbock, V., Teo, K. L., and Jennings, L. S., "A Linear Programming Approach to On-Line Constrained Optimal Terrain-Tracking Systems," *Optimal Control Applications and Methods*, Vol. 14, No. 4, 1993, pp. 229–241.

[9]Barnard, R., "Terrain Tracking Based On Optimal Aim Strategies," *Optimal Control Applications and Methods*, Vol. 15, No. 2, 1994, pp. 145–150.

[10]Zelenka, R. E., Yee, Z., and Zirkler, A., "Flight Test Development and Evaluation of a Kalman Filter State Estimator for Low-Altitude Flight," 2nd Inst. of Electrical and Electronic Engineers Conf. on Control Applications, Vancouver, BC, Canada, Sept. 1993.

[11]Lu, P., "Nonlinear Predictive Controllers for Continuous Systems," *Journal of Guidance, Control, and Dynamics*, Vol. 17, No. 3, 1994, pp. 553–560.

[12]Lu, P., "Optimal Predictive Control of Nonlinear Continuous Systems," *International Journal of Control*, 1995 (to be published).

[13]Lu, P., "Tracking Control of General Nonlinear Systems," Inst. of Electrical Electronics Engineers 33rd Conf. on Decision and Control, Lake Buena Vista, FL, Dec. 1994.

[14]Fletcher, R., *Practical Methods of Optimization*, 2nd ed., Wiley, New York, 1989, Chaps. 8 and 10.

[15]Bryson, A. E., and Desai, M. N., "Energy-State Approximation in Performance Optimization of Supersonic Aircraft," *Journal of Aircraft*, Vol. 6, No. 6, 1969, pp. 481–488.

[16]Pierson, B. L., and Chen, I., "Minimum Altitude-Loss Soaring in a Sinusoidal Vertical Wind Distribution," *Optimal Control Applications and Methods*, Vol. 1, No. 3, 1980, pp. 205–215.